PCCP

Accepted Manuscript

This article can be cited before page numbers have been issued, to do this please use: M. Ziganshin, N. Gubina, A. Gerasimov, V. Gorbatchuk, S. Ziganshina, A. Chuklanov and A. Bukharaev, *Phys. Chem. Chem. Phys.*, 2015, DOI: 10.1039/C5CP03309H.

ROYAL SOCIETY OF CHEMISTRY

www.rsc.org/pccp

View Article Online
DOI: 10.1039/C5CP03309H

Journal Name

ARTICLE

Interaction of L-alanyl-L-valine and L-valyl-L-alanine with organic vapors: thermal stability of clathrates, sorption capacity and change of morphology of dipeptide films

Received 00th January 20xx,
Accepted 00th January 20xx

DOI: 10.1039/x0xx00000x

www.rsc.org/

Marat A. Ziganshin,[a,*] Nadezhda S. Gubina,[a] Alexander V. Gerasimov,[a] Valery V. Gorbatchuk,[a] Sufia A. Ziganshina,[b] Anton P. Chuklanov[b] and Anastas A. Bukharaev[b]

The strong effect of the amino acid sequence in L-alanyl-L-valine and L-valyl-L-alanine on their sorption properties toward organic compounds and water, and the thermal stability of the inclusion compounds of these dipeptides have been found. Generally, L-valyl-L-alanine has a greater sorption capacity for the studied compounds, but the thermal stability of the L-alanyl-L-valine clathrates is higher. Unusual selectivity of L-valyl-L-alanine for vapors of few chloroalkanes was observed. The correlation between the change of the surface morphology of thin film of dipeptides and stoichiometry of their clathrates with organic compounds was found. This discovery may be used to predict the influence of vapors on the morphology of films of short-chain oligopeptide.

Introduction

Bio-friendly and biocompatible materials based on short-chain oligopeptides are being actively investigated owing to their potential use in many different technologies.[1-3] A key feature of the oligopeptides that has caused this high interest is their ability to self-organize with the formation of many structures: nanoparticles[4], nanofibers[5], nanorods[6,7], nanowires[8], nanotubes[9-11], nanospheres[7,12] and dendritic objects.[13] Such nanostructures have been used in sensor systems for the selective detection of neurotoxins[14], as a template for metal nanowires[15] and inorganic nanotubes[16], for the fabrication of composite materials for energy storage devices[17] and microfluidic reactor systems[18], as a transport system for the delivery of DNA into living cells[19], transmembrane channels[20] and for the formation of superhydrophobic surfaces[21], etc.

The type of structure obtained depends on the chemical formula of the oligopeptides[22,23], and the type of solvent used for the crystallization of the nanomaterial[24] or in treating the amorphous film of oligopeptide. It should be noted that the effect of the sequence of the amino acid residues in the oligopeptide[25,26] on the type of nanostructures formed has not been well investigated to date. In the present work, this type of study has been carried out for the dipeptides L-alanyl-L-valine (**AV**) and L-valyl-L-alanine (**VA**).

Another feature of some short-chain oligopeptides is their ability to form crystals with hydrophobic or hydrophilic layers or channels.[22] As a result, these porous crystals have zeolite-like properties[27] and can be used for the selective binding[28], storage[29] or separation of gases.[30,31] The chiral nature of the inert part of the channels in the oligopeptide crystals makes them suitable for the separation of racemic mixtures.[22,32]

However, it should be noted that the *soft nature*[33,34] of the oligopeptide crystals may cause solvent-induced single-crystal-to-single-crystal transformations[35] or destruction of the crystal after binding organic molecules[36]. This complicates the study of the sorption properties of oligopeptide materials. However, this behavior can also be used to control the self-organization of oligopeptides in the solid phase to produce nanomaterials with more desirable properties. In this work, we carried out a comprehensive study of the interaction of L-alanyl-L-valine and L-valyl-L-alanine in the systems that combine solid oligopeptides with the vapors of water or an organic compound.

Previously, these dipeptides have been shown to form crystals with spiral channels with diameters of 5.36 Å and 5.08 Å for L-alanyl-L-valine and L-valyl-L-alanine, respectively, giving a total empty space in the crystal of 10.90%.[37] L-Alanyl-L-valine bound xenon[29], methanol[38,39], acetonitrile[39], isopropanol[39], toluene[38], carbon dioxide[28] and methane[28], whereas L-valyl-L-alanine bound xenon[29], methane[28], carbon dioxide[28] and acetonitrile[40]. It should be noted that despite the **AV** and **VA** crystals having the same crystal system with similar cell parameters[37], their sorption properties differed.[28,29]

In the present work, the sorption of organic vapors or water by a dipeptide layer was studied on a quartz crystal microbalance (QCM-sensor). The results were used to analyze the structure-property relationships of this process. The thermal stability of the products of dipeptide saturation with vapors was studied using

[a.] A.M. Butlerov Institute of Chemistry, Kazan Federal University, Kremlevskaya ul. 18, Kazan, 420008 Russia.
[b.] Kazan Zavoisky Physical-Technical Institute of the Kazan Scientific Center of the Russian Academy of Sciences, Sibirskii trakt 10/7, Kazan, 420029 Russia.
† Electronic Supplementary Information (ESI) available: TG/DSC/MS data for the studied dipeptides and products of their saturation with guest vapors; AFM images of the surface of thin film of dipeptide saturated with vapors. See DOI: 10.1039/x0xx00000x

View Article Online
DOI: 10.1039/C5CP03309H

thermogravimetric (TG) analysis with simultaneous differential scanning calorimetry (DSC) and mass-spectrometric (MS) detection of the evolved vapors. Changes in the surface morphology of the thin layers of dipeptides treated with vapors were observed by atomic force microscopy (AFM).

Experimental

Materials

Dipeptides $_L$-alanyl-$_L$-valine (**AV**) (Bachem, №G-1420.0001) and $_L$-valyl-$_L$-alanine (**VA**) (Bachem, №G-3500.0001) were used without additional purification.

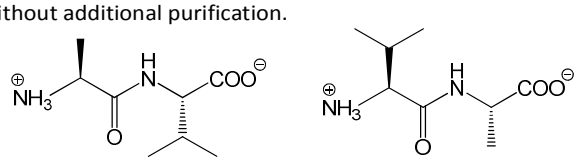

AV **VA**

Purified organic guests[41] had at least 99.5% purity.

QCM study of guest binding

A sensor device with 10 MHz QCM crystals (Part No. 151620-10, ICM Co. Inc, USA) of thickness shear mode (TSM) was used.[42] The dipeptide coatings (~0.65 µg) were prepared by drop and drying (for 2 min) by hot air (45°C) of methanol solution on the gold surface of quartz crystals. These coatings with an average thickness 40 nm give a decrease of ΔF ~ 800 Hz in the crystal frequency after solvent removal. The thickness value was estimated by the layer area, mass and density of **AV** and **VA** ρ = 1.033 g/cm^3 and ρ = 1.027 g/cm^3, respectively, calculated from X-ray single crystal data.[29]

In a QCM sensor experiment, a liquid guest (sorbate) was sampled using microsyringe to the sensor cell bottom through a dosing hole in the cell cover. The sampled guest amount was twice as large as necessary to create a saturation vapor in the sealed cell. Still, the cell was made not hermetical during sensor experiment to avoid guest condensation on the coating surface. The guest relative vapor pressure P/P_0 was kept below saturation level by the vapor leak through the dosing hole. This level is equal to P/P_0 = 0.85[43]. A sensor baseline noise did not exceed 3 Hz. The frequency change of quartz crystal ΔF in sensor experiments was determined with the reproducibility of 5% for ΔF > 50 Hz. The stoichiometry of host-guest clathrates was determined using QCM sensor method with the error of 10%.

To regenerate the dipeptide coatings after the guest binding, they were dried by hot air as described above. This regeneration procedure was repeated at least twice until the constant sensor frequency was achieved. In most cases such procedure gave the value of frequency change corresponding to initial coating prepared from the methanol solution. The residual water content in this coating, determined as describe elsewhere[36], does not exceed 0.5% w/w.

Thermoanalysis by Simultaneous TG/DSC/MS

Simultaneous thermogravimetry (TG) and differential scanning calorimetry (DSC) analysis of dipeptide powder with mass spectrometric (MS) evolved gas analysis were performed using thermoanalyzer STA 449 C Jupiter (Netzsch) coupled with quadrupolar mass-spectrometer QMS 403C Aeolos (Netzsch) as described elsewhere[42,44]. In each experiment, the temperature rate was 10 K/min, and an argon atmosphere with a total flow rate of 75 ml/min was used. For this experiment, 5-7 mg samples of guest-free dipeptide were placed in aluminum crucibles (40 µl) with lids having 3 holes, each of 0.5 mm in diameter. The samples of dipeptide saturated with water or organic vapors were prepared in the same crucibles by equilibration with vapors of these guests (P/P_0=1) for 72 h at 25°C in hermetically sealed 15 ml vials. The TG/DSC/MS experiment began after 20 minutes of their equilibration at 25°C in argon flow of 75 ml/min. The sample mass loss was determined with the error of 5 %.

Atomic force microscopy (AFM)

AFM images in topography and phase modes were recorded using the atomic force microscope Solver P47 (NT-MDT, Russia).[36,45] Measurements were performed in air using a tapping mode. Standard silicon cantilevers NSG-11 (NT-MDT, Russia) were used. For AFM experiments, dipeptide films with diameter of 3 mm were prepared on the surfaces of highly oriented pyrolytic graphite (HOPG) plates (1×1 cm) using the same technique as for QCM study. HOPG was freshly cleaved before use. In these experiments, first, an AFM image was obtained for the initial dipeptide film dried from methanol solvent. Then the dipeptide layer was saturated with water or organic vapors. Thereafter, the guest was removed from the dipeptide as described above for sensor experiment, and the AFM image of the film was obtained.

Results and discussion

The QCM sensor responses (ΔF) of the quartz crystals coated with **AV** or **VA** were determined for the vapors of 22 organic guests and water at a relative vapor pressure of P/P_0 = 0.85 at 298 K. Typical sensor responses for the guest vapors are given in Fig. 1 and 2.

The equilibration time for this experiment was in the range from 110 s for the sorption of ethanol on **VA** (Fig. 2) to more than 10,000 s for the sorption of *n*-hexane on **AV** (Fig. 1).

The guest/host molar ratio S (Table 1) was calculated using the equation:

$$S = (\Delta F / \Delta F_{\text{dipeptide}}) \times (M_{\text{dipeptide}} / M_{\text{guest}})$$

where $\Delta F_{\text{dipeptide}}$ is the frequency change corresponding to the dipeptide mass, and $M_{\text{dipeptide}}$ and M_{guest} are the molar weights of dipeptide and guest, respectively. The observed values of

View Article Online
DOI: 10.1039/C5CP03309H

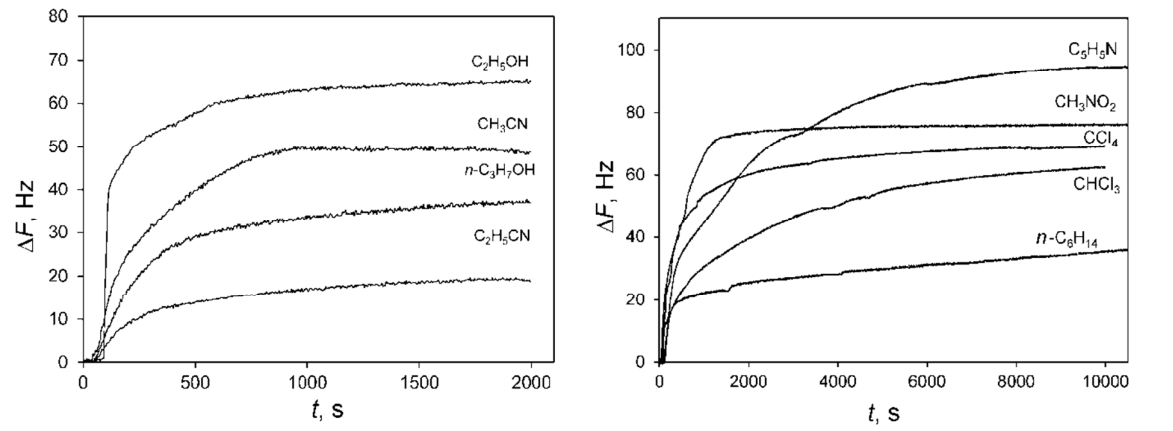

Fig. 1. Responses of QCM sensor coated with dipeptide **AV** to organic vapors with relative vapor pressure P/P_0 = 0.85 at T = 298 K. Sensor responses ΔF are normalized to the coating mass with corresponding frequency decrease of $\Delta F_{dipeptide}$ = 800 Hz.

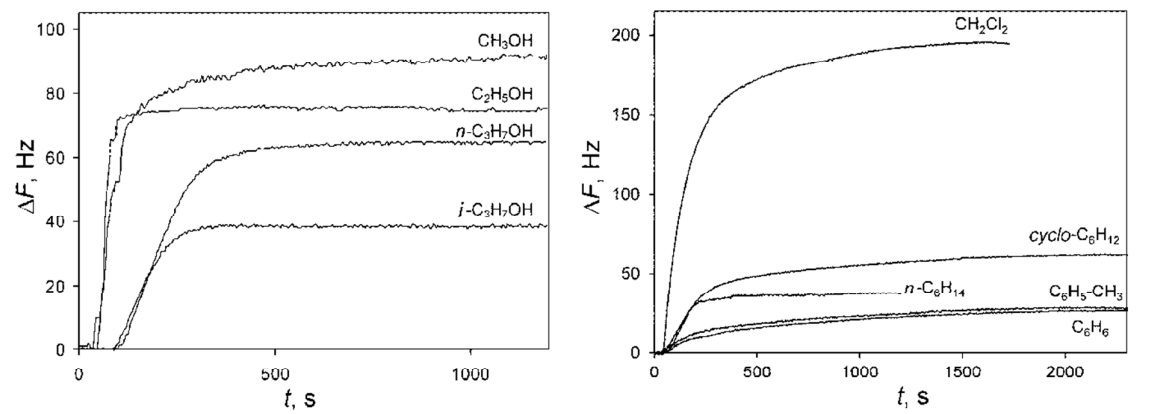

Fig. 2. Responses of QCM sensor coated with dipeptide **VA** to organic vapors with relative vapor pressure P/P_0 = 0.85 at T = 298 K. Sensor responses ΔF are normalized to the coating mass with corresponding frequency decrease of $\Delta F_{dipeptide}$ = 800 Hz.

the guest content (S) in **AV** that was saturated with methanol, isopropanol and acetonitrile (Table 1) were less than the guest content calculated from single crystal XRD data for the corresponding inclusion compounds.[39] These differences may have been caused by the dipeptides forming inclusion compounds with different guest content depending on the method of preparation. For example, in this work, the product of **VA** saturation with acetonitrile (Table 1) has an intermediate composition when compared with the acetonitrile content in the two different clathrates with **VA**, which were prepared in different ways.[40] In the last case the content of acetonitrile decreases from 0.33 to 0.12 mol guest per mol **VA** when the monoclinic structure irreversibly converted to a hexagonal polymorph upon drying.

A general picture of the selectivity of the dipeptides for specific guest vapors may be seen in the correlation between the stoichiometry of the complexes and the guest molar refraction MR_D, Fig. 3. MR_D is a good parameter to describe molecular size[47,48]. The sorption capacity of **AV** and **VA** for the vapors of the studied arenes, linear alcohols, alkanes and nitriles (C_1-C_2) decreases with each added methylene group. The S value for most studied guests with a MR_D greater than 16 cm^3/mol (**AV**) and 20 cm^3/mol (**VA**) does not exceed 0.2 mol guest per mol dipeptide (Fig. 3). The exception is clathrates of **AV** with pyridine, and **VA** with pyridine, chloroform and dichloromethane (Fig. 3 and Table 1). The higher sorption capacity of the dipeptides for these guests may be because of their ability to form H-bonds with the host or more effective packing in the solid phase.

VA is more selective towards some of the studied guests than **AV**. **AV** generally has the same sorption capacity for the guests with similar sizes, like C_2H_5OH, CH_3CN, CH_3NO_2, while **VA** binds twice as much ethanol as similar-sized H-acceptors (Fig. 3 and Table 1).

Both dipeptides **AV** and **VA** were more selective for n-propanol than isopropanol (Fig. 3, and Table 1), a trend that has been seen previously in the selectivity of the tripeptide $_L$-leucyl-$_L$-leucyl-$_L$-leucine[36], some proteins[49,50], polymer[51] and dendrimer[52] towards these isomers. This difference in selectivity is clearly related to shape of alcohol molecules. The linear n-propanol better fills the narrow channels in dipeptide phase.

View Article Online
DOI: 10.1039/C5CP03309H

Table 1 The guest/host molar ratio calculated from QCM sensor data

№	Guest	MR_D[a] (cm^3/mol)	*S* (mol guest/ mol **AV**)	*S* (mol guest/ mol **VA**)
1	H_2O	3.7	0.67	0.60
2	CH_3OH	8.3	0.67[b] (0.75)[c]	0.69
3	C_2H_5OH	13.0	0.30	0.38
4	*n*-C_3H_7OH	17.5	0.15	0.24
5	*i*-C_3H_7OH	17.6	0.10 (0.25)[c]	0.15
6	*n*-C_4H_9OH	22.1	0.09	0.09
7	CH_3CN	11.1	0.29 (0.35)[c]	0.21 (0.12; 0.33)[d]
8	C_2H_5CN	16.0	0.08	0.18
9	C_3H_7CN	20.4	0.09	0.07
10	C_4H_9CN	25.2	0.08	0.05
11	*cyclo*-C_6H_{12}	27.7	0.10	0.18
12	*n*-C_6H_{14}	29.9	0.10	0.10
13	*n*-C_7H_{16}	34.5	0.08	0.09
14	CH_2Cl_2	16.4	0.11	0.54
15	$CHCl_3$	21.3	0.12	0.82
16	CCl_4	26.4	0.11	0.10
17	C_6H_6	26.3	0.11	0.08
18	$C_6H_5CH_3$	31.1	0.08[b]	0.07
19	C_5H_5N	24.2	0.28	0.77
20	CH_3NO_2	12.5	0.29	0.19
21	$(CH_3)_2CO$	16.2	0.11	0.17
22	THF	19.9	0.16	0.25

[a] $MR_D = (M/d)\times(n_D^2 - 1)/(n_D^2 + 2)$, where *M* is molecular weight of guest, *d* and n_D are density and refractive index of liquid guest, respectively; [b] data from[46]; [c] X-ray data from[39]; [d] X-ray data from[40].

The effect of the sequence of the amino acid residues in the dipeptide on its sorption capacity towards the studied compounds is seen in the *S* vs. MR_D plot (Fig. 4). For clathrates with S ≥ 0.1 (mol guest per mol dipeptide) the sorption capacity of **VA** is higher in most cases. **AV** binds only water, acetonitrile and nitromethane more than the **VA** at 12%, 38% and 53%, respectively. This is surprising because the channel diameter in crystals of **AV** is greater than in **VA**, and the free volume in the two crystals is almost identical[29]. However, these data are in agreement with the ability of **VA** to bind greater volumes of gases than **AV**[27,28]. One could suppose that **VA** has more flexible packing, which can change during the sorption process and thereby increase the available volume.

These experiments showed that the dipeptides **AV** and **VA** bind reversibly all studied guests, except for CCl_4 (**AV**) and pyridine (**VA**). However, the sorption capacity of **AV** was only completely restored after removal of water, methanol, nitromethane, ethanol, propionitrile, *n*-hexane, acetone and THF. For **VA**, removal of methanol, nitromethane, ethanol, propionitrile, butyronitrile, valeronitrile, benzene, cyclohexane, toluene, acetone and THF lead to a complete recovery of the sorption capacity. In other cases, a significant decrease of sorption capacity was observed after the regeneration of the sensors.

We have studied the decomposition of clathrates of dipeptides with water and organic guests that are stable at RT by TG/DSC/MS analysis (Fig. 5, 6, and ESI†). All of the studied clathrates lose the guest in a single step over a wide

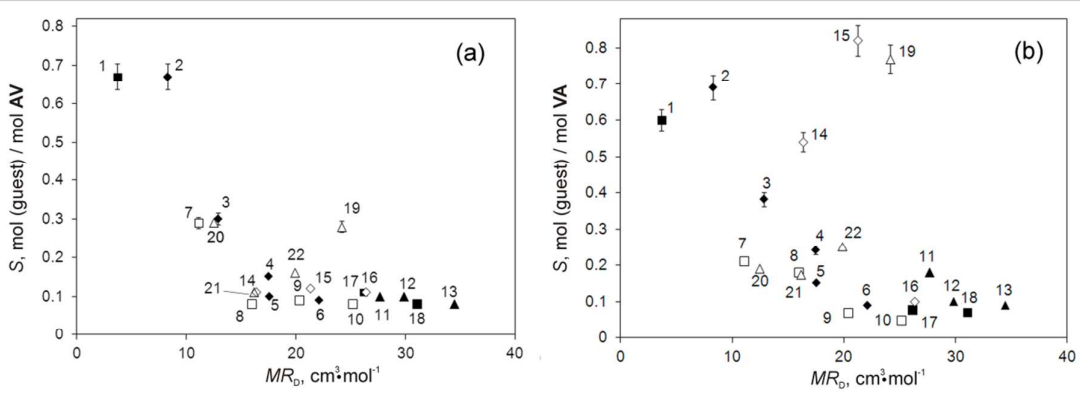

Fig. 3. Correlation of the guest/host molar ratio *S* in inclusion compounds of **AV** (a) and **VA** (b) with guest molar refraction MR_D. Point numbers correspond to the guest numbers in Table 1.

View Article Online
DOI: 10.1039/C5CP03309H

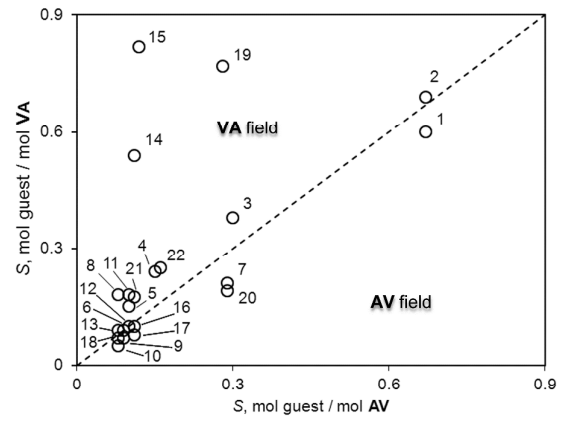

Fig. 4. Correlation between guest/host molar ratios *S* of inclusion compounds of **AV** and **VA**. Point numbers correspond to the guest numbers in Table 1.

temperature range, except for the clathrate **VA** with pyridine. The obtained DSC curves do not exhibit any polymorphic phase transitions, except for the clathrate **AV** with water. In this case (Fig. 5a) an endothermic peak of ~4 kJ/mol at 211°C was observed. Because there is no change in the sample mass, one can assume that there has been a change in the phase of the dipeptide[54]. **AV** decomposes above 220°C and **VA** above 190°C (ESI†).

The results of the thermoanalysis are given in Table 2 including the mass loss (Δm), composition of the clathrates (S_{TG}) and DTG temperatures (differential TG) peaks (T_{max}). According to the obtained data, most clathrates lose part of the bound guest during pre-equilibration at room temperature before the thermal analysis. The exceptions are the clathrates of **AV** with chloroalkanes for which, the guest content calculated from data of thermal analysis was higher than the stoichiometry from the sensor analysis, and the clathrate **VA** with CCl_4 had a S_{TG} that was close to *S*, Table 1 and 2.

The composition of most of the studied clathrates was in the range of 0.15–0.20 mol guest per mol dipeptide (Table 1). We found no simple correlation between the size of the guest molecule and the stoichiometry of the clathrate. Generally, the guest content is higher in the clathrates of **AV**. Only the **VA**•0.17CH_3CN and **VA**•0.37C_5H_5N clathrates had S_{TG} values greater that the corresponding **AV** clathrates, at 1.2 and 1.7 times more, respectively.

If the T_{max} value is used as a metric for the thermal stability of the clathrates, then **AV** forms the more stable inclusion compounds, except for clathrates with pyridine and methylene chloride (Fig. 7). For methylene chloride, the DTG-peaks of the decomposition of the **AV** and **VA** clathrates occur at the same temperature. The clathrate **VA** with pyridine is the most stable inclusion compound of the two dipeptides (Fig. 7). The decomposition of this clathrate occurs cooperatively over a narrow range of temperatures (Fig. 6d). The difference between the T_{max} and the boiling point of pyridine is 28°C. A temperature deviation previously seen for clathrates of L-leucyl-L-leucyl-L-leucine with pyridine, in which the organic compound forms a H-bond with the tripeptide, is about 30°C. Thus, we can expect H-bonds to be involved in the **VA**•0.37C_5H_5N clathrate.

The low stability of the clathrates **AV** with methanol and **VA** with methanol show that methanol is a good solvent for the preparation of dipeptide thin films. It may also be useful in the exchange of irreversibly bonded guests.[42,52]

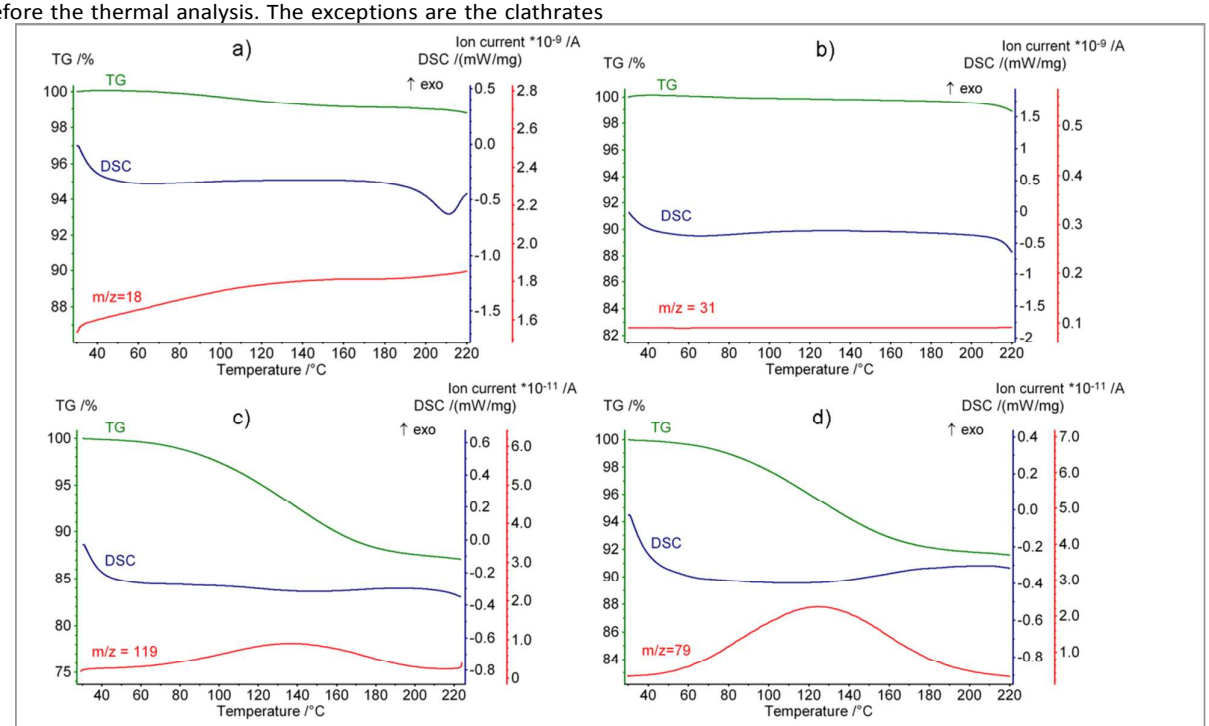

Fig. 5. The data of TG/DSC/MS analysis for product of dipeptide **AV** saturation with vapor of (a) water, (b) methanol, (c) carbon tetrachloride and (d) pyridine. Ion thermograms of H_2O (m/z=18), CH_3OH (m/z=31), CCl_4 (m/z=119) and C_5H_5N (m/z=79) are shown. Heating rate is 10 K/min.

View Article Online
DOI: 10.1039/C5CP03309H

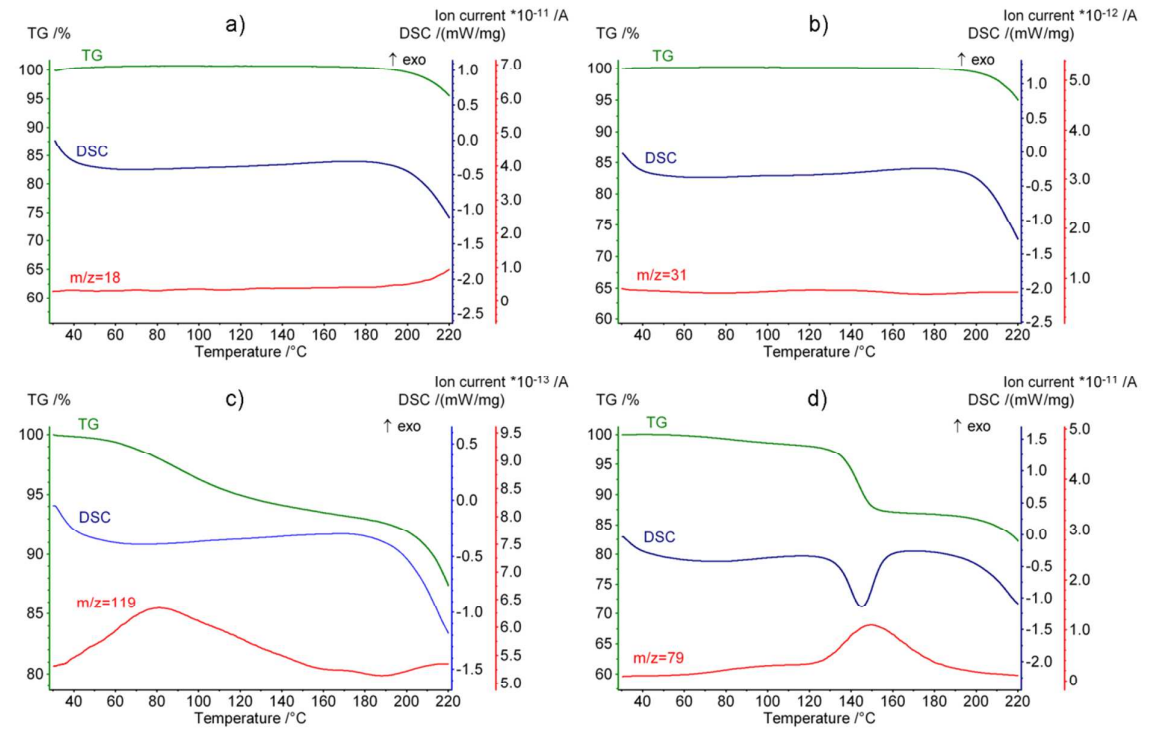

Fig. 6. The data of TG/DSC/MS analysis for product of dipeptide **VA** saturation with vapor of (a) water, (b) methanol, (c) carbon tetrachloride and (d) pyridine. Ion thermograms of H_2O (m/z=18), CH_3OH (m/z=31), CCl_4 (m/z=119) and C_5H_5N (m/z=79) are shown. Heating rate is 10 K/min.

The same techniques used in the preparation of the dipeptide thin films for sensor analysis were used in an AFM study on the effect of the vapors on the morphology of the films. AFM images of the initial film of these dipeptides (Fig 8a and 9a) and the same films after saturation with vapors were obtained (Fig. 8, 9, and ESI†). Smooth films of dipeptides are formed on surface of HOPG after solvent (methanol) has been removed. The average height spread on a 5×5-µm scan was 9 nm for **AV** and 7 nm for **VA**. A mean square roughness of the surface (R_q) was 0.95±0.05 and 0.96±0.05 nm for **AV** and **VA** films, respectively.

We have found that the compounds used for saturation of dipeptide films can be divided into three groups according to their effect on morphology of film surface: no influence, weak effects, and strong effects. These groups are the same compounds for the two dipeptides, except for *n*-hexane. *n*-

Table 2 The data of simultaneous TG/DSC/MS analysis of clathrates prepared by saturation of **AV** and **VA** with vapors of organic guests and water.

Guest	**AV**			**VA**		
	Δ*m* (%)	S_{TG}, mol guest/mol **AV**	T_{max}, °C	Δ*m* (%)	S_{TG}, mol guest/mol **VA**	T_{max},°C
H_2O	0.9	0.09	111	-[c]	-	-[b]
CH_3OH	0.4[a]	0.02	-[b]	-[c]	-	-[b]
CH_3CN	3.1	0.15	81	3.6	0.17	73
CH_3NO_2	4.2	0.14	111	4.3	0.14	78
C_2H_5OH	4.7	0.20	108	1.1	0.05	-
CH_2Cl_2	8.1	0.19	97	6.8	0.16	96
$CHCl_3$	10.5	0.18	91	8.8	0.15	78
C_5H_5N	8.4	0.22	121	13.5	0.37	143
CCl_4	12.2	0.17	98	7.2	0.09	90

[a] error is 10%; [b] T_{max} cannot be determined; [c] mass lose is less than experimental error

View Article Online
DOI: 10.1039/C5CP03309H

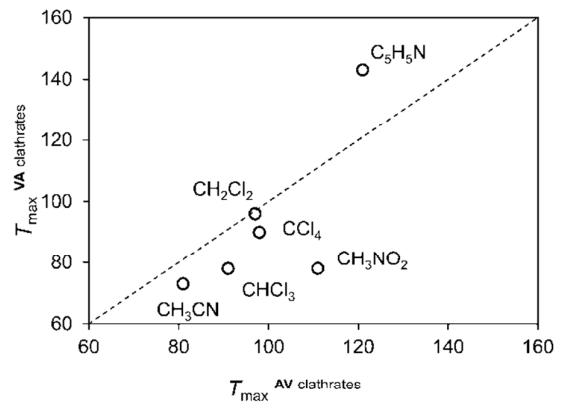

Fig. 7. The relationship between the values of T_{max} (temperature of DTG-peak) for **AV** and **VA** clathrates.

Hexane had no influence on **AV** and weak effects on **VA**.

After the saturation of **AV** and **VA** films with nitromethane vapor, their morphology does not change (Fig 9b and ESI†). The calculated R_q was 1.3±0.2 nm for **AV** and 0.85±0.1 nm for **VA** (Fig 8 and 9). Also, no significant changes in the morphology of **VA** film saturated with water vapors were observed, ESI†. The average height spread on a 5×5-µm scan was 2.5 nm and the R_q was 0.34±0.03 nm.

The effects of *n*-hexane vapor on the morphologies of the **AV** and **VA** films were found to be significantly different (ESI†). For **AV**, an R_q=1.21±0.2 nm meant the surface was practically unchanged. While the interaction of **VA** with *n*-hexane vapor led to the formation of the small particles with an average diameter of 0.3–0.5 µm and a height 15–25 nm above the surface. The R_q=3.65±0.05 nm is more than three times that of the initial film. This may be due to partial swelling and delamination of the film.

The saturation of **VA** film as well as **AV** film[38] with methanol vapor leads to the formation of small objects (weak effect) along the crystallographic steps of the pyrolytic graphite (Fig. 9c) with an R_q=1.99±0.02 nm for the **VA** film. In a 5×5-µm scan, 44 particles with lengths of 300-400 nm, widths of 150–230 nm and heights 5–14 nm were found. The square of particles formed after interaction of **VA** with methanol vapor is more than ten times that in case of **AV** particles formed in the same conditions.

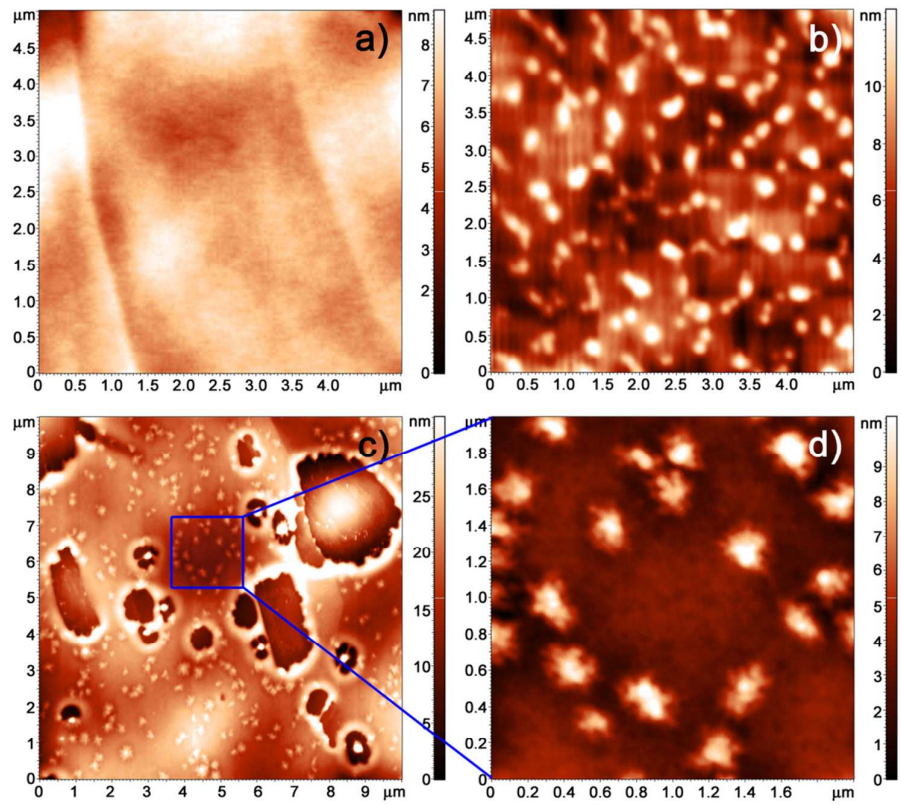

Fig. 8. AFM images of the surface of (a) the initial **AV** film deposited on HOPG surface from a methanol solution; the film saturated with vapors of (b) pyridine for 2 h, (c) and (d) methylene chloride for 75 min, T=298K. Before AFM experiment all films were dried by hot air (45°C) for 2 min.

View Article Online
DOI: 10.1039/C5CP03309H

The interaction of the **VA** film with toluene vapors led to the formation of a porous surface of dipeptide film (strong effect), as seen in Fig.9d, with an R_q=0.92±0.1 nm. The pores had diameters from 20 to 200 nm, and the average height spread on a 5×5-µm scan was 7 nm. The effect of toluene on the morphology of **VA** film was unique and quite different from the effect on the **AV** film. Toluene vapors cause the formation of objects 80–180 nm in diameter and 2–15 nm in

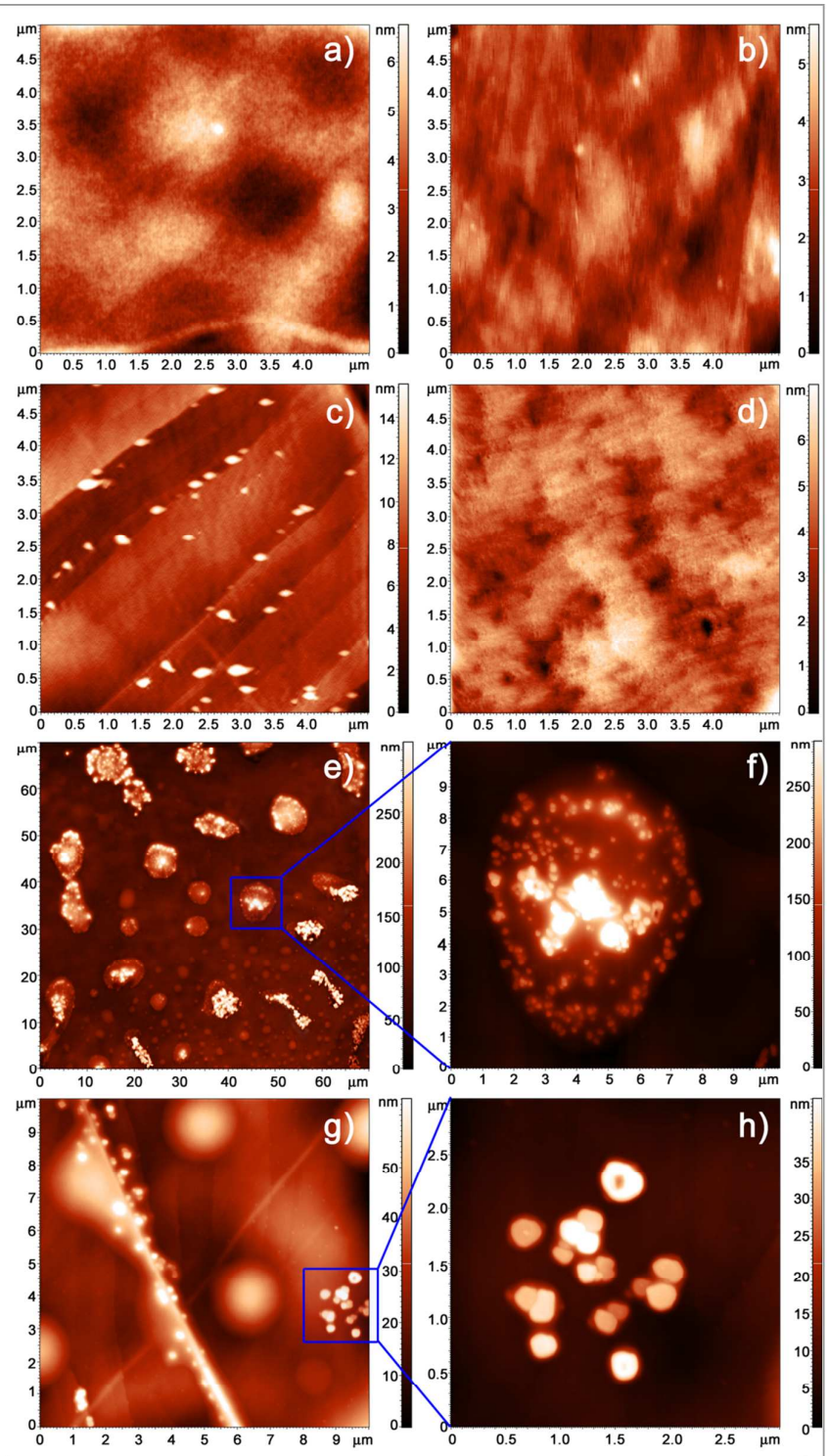

Fig. 9. AFM images of the surface of (a) the initial **VA** dipeptide film deposited on HOPG from a methanol solution; the film saturated with vapors of (b) nitromethane for 50 min; (c) methanol for 20 min; (d) toluene for 25 min; (e) and (f) methylene chloride for 75 min; (g) and (h) chloroform for 60 min, T=298K. Before AFM experiment all films were dried by hot air (45°C) for 2 min.

View Article Online
DOI: 10.1039/C5CP03309H

height on the **AV** film.[38]

A significant change in the morphology of the **AV** film was observed after the binding of pyridine vapor (Fig. 8b). Nanostructures 80–320 nm in diameter (180 is more often) and 5–7 nm height were formed. On a 5×5-µm scan 137 particles were found. The mean square roughness of the surface increased by 50% over the initial value to R_q=2.3±0.2 nm. For **VA**, well-shaped oblong nanostructures with narrowed ends were formed during the interaction with pyridine vapor.[53]

After saturation of the **AV** film with methylene chloride vapor, numerous particles with lateral size of 80–220 nm and height of 2–10 nm were formed (Fig. 8c). Around these particles there were dendritic branches (Fig. 8d) typical for nonequilibrium crystallization processes, where the nutrition of the crystals was limited[55]. This surface gave an *R*q of 1.75 nm for a 2×2 µm image (5.67 nm for a 10×10-µm image). It should be noted that the holes were already present on the initial film (*R*q=3.84 nm for a 10×10-µm image, ESI†).

The saturation of the **VA** film with methylene chloride vapor led to the formation of two types of objects. First, complex agglomerates with clear boundaries formed with lateral sizes of about 5–10 µm (Fig. 9e). These large objects are composed of many smaller particles 70–400 nm in diameter and 30–200 nm in height (Fig. 9f). Second, there were more spherical particles 0.8–4 µm in diameter and 20–100 nm in height. On the surface of some of them, objects similar to those on the surface of big agglomerates could be found (ESI†). Thus, it appears the spheroids are progenitors of the more complex structures. It should be noted that in the system **VA**/CH_2Cl_2 formed the highest dipeptide structures of those studied here. This may be due to the high solubility of **VA** in the saturated vapor of methylene chloride.

We also studied the effect of chloroform vapor on film morphology of **VA**, which binds this organic compound in large quantities according to the QCM data (Table 1). After saturation of the initially smooth film with chloroform for 1 hour, two types of objects were found on the surface. First, large spherical formations 2–4 µm in diameter and 17–105 nm in height (Fig. 9g and ESI†) were formed. The second type of objects were 120–500 nm in diameter and 20–40 nm in height and were located mainly along the crystallographic steps of the HOPG and in the regions of the film that were free from the large formations (Fig. 9h and ESI†). Some of them had regular, crystalline shapes.

Conclusions

The sorption properties of $_L$-alanyl-$_L$-valine (**AV**) and $_L$-valyl-$_L$-alanine (**VA**) toward water and organic vapors were studied using piezoelectric sensors. The sorption capacity of these dipeptides was found to have a non-linear dependence on the size of guest molecules. A strong "size exclusion" effect was observed for the binding of organic compounds larger than methanol, which increased with the molecular size of the guest. On the other hand, **AV** was selective for pyridine, and **VA** was selective for chloroform, methylene chloride and pyridine. Generally, **AV** formed more thermal stable clathrates at lower guest contents than **VA**. The exception is the clathrate **VA** with pyridine. In this case we suppose that the H-bond between the dipeptide and organic compound caused the difference. The changes in morphology of the thin films of **AV** and **VA** after guest binding were observed directly by atomic force microscopy. Using QCM and AFM, relatively small molecules (H_2O and methanol) were found to be capable of effectively binding with **AV** and **VA** without essential change in the dipeptide packing in the solid phase. Organic compounds with a MR_D greater than 13 cm^3mol^{-1}, even where the capacity of the dipeptide for the molecule was not large, could change the surface morphology of the dipeptide films. The shape and size of the nano- and micro-objects that formed on the surface of the films strongly depends on the size and physical-chemical properties of organic compound and the structure of the dipeptide.

Acknowledgements

This study was supported by the Russian Foundation for Basic Research, Project No. 12-03-00590-a and Russian Government Program of Competitive Growth of Kazan Federal University.

References

1 J. J. Panda and V. S. Chauhan, *Polym. Chem.*, 2014, **5**, 4418–4436.
2 E. Gazit, *Chem. Soc. Rev.*, 2007, **36**, 1263–1269.
3 H. Tsutsumi and H. Mihara, *Mol. BioSyst*, 2013, **9**, 609–617.
4 L. Sun, Z. Fan, Y. Wang, Y. Huang, M. Schmidt and M. Zhang, *Soft Matter*, 2015, **11**, 3822–3832.
5 A. Mahler, M. Reches, M. Rechter, S. Cohen and E. Gazit, *Adv. Mater.*, 2006, **18**, 1365–1370.
6 J. Ryu and C.B. Park, *Chem. Mater.*, 2008, **20**, 4284–4290.
7 C. Guo, Y. Luo, R. Zhou and G. Wei, *Nanoscale*, 2014, **6**, 2800–2811.
8 J. Ryu and C.B. Park, *Adv. Mater.*, 2008, **20**, 3754–3758.
9 I. W. Hamley, *Angew. Chem. Int. Ed.*, 2014, **53**, 6866–6881.
10 M. Wang, L. Du, X. Wu, Sh. Xiong and P.K. Chu, *ACS Nano*, 2011, **5**, 4448–4454.
11 S. Ray, D. Haldar, M. G. B. Drew, and A. Banerjee, *Org. Lett.*, 2004, 6, 4463–4465.
12 M. Sakurai, P. Koley and M. Aono, *Chem. Commun.*, 2014, **50**, 12556–12559.
13 V. V. Korolkov, S. Allen, C. J. Roberts and S. J. B. Tendler, *Faraday Discuss.*, 2013, **166**, 257–267.
14 J. H. Kim, J. Ryu and C. B. Park, *Small*, 2011, **7**, 718–722.
15 M. Reches and E. Gazit, *Science*, 2003, **300**, 625–627.
16 J. Ryu, S. W. Kim, K. Kang and C. B. Park, *Adv. Mater*, 2010, **22**, 5537–5541.
17 J. Ryu, S.-W. Kim, K. Kang and C. B. Park, *Acs Nano*, 2010, **4**, 159–164.
18 H.-I. Ryoo, J. S. Lee, C. B. Park, D.-P. Kim, *Lab Chip*, 2011, **11**, 378–380.
19 X. Yan, Q. He, K. Wang, L. Duan, Y. Cui and J. Li, *Angew. Chem. Int. Ed.*, 2007, **46**, 2431–2434.
20 J. Sa´nchez-Quesada, M. P. Isler, and M. Reza Ghadiri, *J. Am. Chem. Soc.*, 2002, **124**, 10004–10005.
21 J. S. Lee, J. Ryu and C. B. Park, *Soft Matter*, 2009, **5**, 2717–2720.
22 C. H. Görbitz, *Chem. Eur. J.*, 2007, **13**, 1022–1031.

View Article Online
DOI: 10.1039/C5CP03309H

23 P. Tamamis, L. A. Abramovich, M. Reches, K. Marshall, P. Sikorski, L. Serpell, E. Gazit and G. Archontis, *Biophysical Journal*, 2009, **96**, 5020–5029.
24 K. Ariga, J. Kikuchi, M. Naito, E. Koyama and N. Yamada, *Langmuir*, 2000, **16**, 4929–4939.
25 M. A. Ziganshin, I. G. Efimova, V. V. Gorbatchuk, S. A. Ziganshina, A. P. Chuklanov, A. A. Bukharaev and D. V. Soldatov, *J. Peptide Sci.*, 2012, **18**, 209–214.
26 J. Ryu and C. B. Park, *Biotechnol. Bioeng.*, 2010, **105**, 221–230.
27 R. Afonso, A. Mendes and L. Gales, *Journal of Materials Chemistry*, 2012, **22**, 1709–1723.
28 A. Comotti, S. Bracco, G. Distefano and P. Sozzani, *Chem. Commun*., 2009, 284–286.
29 D. V. Soldatov, I. L. Moudrakovski and J. A. Ripmeester, *Angew. Chem. Int. Ed.*, 2004, **43**, 6308–6311.
30 R. V. Afonso, J. Durão, A. Mendes, A. M. Damas and L. Gales, *Angew. Chem. Int. Ed*. 2010, **49**, 3034–3036.
31 A. Comotti, A. Fraccarollo, S. Bracco, M. Beretta, G. Distefano, M. Cossi, L. Marchese, C. Riccardi and P. Sozzani, *CrystEngComm.*, 2013, **15**, 1503–1507.
32 T. J. Burchell, D. V. Soldatov and J. A. Ripmeester, *J. Struct. Chem.*, 2008, **49**, 188–191.
33 W. Hamley, *Angew. Chem. Int. Ed.*, 2003, **42**, 1692–1712.
34 H. Zhang, K. Siegrist, D. F. Plusquellic and S. K. Gregurick, *J. Am. Chem. Soc.*, 2008, **130**, 17846–17857.
35 S. Guha, M. G. B. Drew and A. Banerjee, *CrystEngComm*., 2009, **11**, 756–762.
36 M. A. Ziganshin, I. G. Efimova, V. V. Gorbatchuk, S. A. Ziganshina, A. P. Chuklanov, A. A. Bukharaev and D.V. Soldatov, *J. Peptide Sci.*, 2012, **18**, 209–214.
37 D. V. Soldatov, I. L. Moudrakovski, E. V. Grachev and J. A. Ripmeester, *J. Am. Chem. Soc.*, 2006, **128**, 6737–6744.
38 I. G. Efimova, M. A. Ziganshin, V. V. Gorbatchuk, D. V. Soldatov, S. A. Ziganshina, A. P. Chuklanov and A. A. Bukharaev, *Prot. Met. Phys. Chem. Surf.*. 2009, **45**, 525–528.
39 C. H. Görbitz, *Acta Crystallogr., Sect. B: Struct. Sci.,* 2002, **58**, 849–854.
40 C. H. Görbitz, *CrystEngComm*., 2005, **7**, 670–673.
41 W. L. F. Armarego and C. L. L. Chai, *Purification of laboratory chemicals*, Oxford, Butterworth-Heinemann, UK, 2009.
42 L. S. Yakimova, M. A. Ziganshin, V. A. Sidorov, V. V. Kovalev, E. A. Shokova, V. A. Tafeenko, V. V. Gorbatchuk, J. *Phys. Chem. B*, 2008, **112**, 15569–15575.
43 G. D. Safina, L. R. Validova, M. A. Ziganshin, I. I. Stoikov, I. S. Antipin and V. V. Gorbatchuk, *Sens. Actuators, B*, 2010, **148**, 264–268.
44 K. V. Gataullina, M. A. Ziganshin, I. I. Stoikov, A. T. Gubaidullin and V. V. Gorbatchuk, *Phys. Chem. Chem. Phys.*, 2015, **17**, 15887–15895.
45 M. A. Ziganshin, A. A. Bikmukhametova, A. V. Gerasimov, V. V. Gorbatchuk, S. A. Ziganshina and A. A. Bukharaev, *Prot. Met. Phys. Chem. Surf.*, 2014, **50**, 49–54.
46 I. G. Efimova, M. A. Ziganshin, V. V. Gorbatchuk, D. V. Soldatov, S. A. Ziganshina, A. P. Chuklanov and A. A. Bukharaev, *Prot. Met. Phys. Chem. Surf.* 2009, **45**, 525–528.
47 M. A. Ziganshin, A. V. Gerasimov, V. V. Gorbatchuk and A. T. Gubaidullin, *J. Therm. Anal. Calorim.*, 2015, **119**, 1811–1816.
48 B. N. Solomonov and A. I. Konovalov, *Russ. Chem. Rev.*, 1991, **60**, 45–68.
49 V. V. Gorbatchuk, M. A. Ziganshin and B. N. Solomonov, *Biophys. Chem.*, 1999, **81**, 107–123.
50 V. V. Gorbatchuk, M. A. Ziganshin, N. A. Mironov and B. N. Solomonov, *Biochim. Biophys. Acta*, 2001, **1545**, 326–338.
51 V. V. Gorbatchuk, N. A. Mironov, B. N. Solomonov and W. D. Habicher, *Biomacromolecules*, 2004, **5**, 1615–1623.
52 A. V. Gerasimov, M. A. Ziganshin, A. E. Vandyukov, V. I. Kovalenko, V. V. Gorbatchuk, A-M. Caminade and J-P. Majoral, *J. Colloid Interface Sci.*, 2011, **360**, 204–210.
53 M. A. Ziganshin, I. G. Efimova, A. A. Bikmukhametova, V. V. Gorbachuk, S. A. Ziganshina, A. P. Chuklanov and A. A. Bukharaev, *Prot. Met. Phys. Chem. Surf.*, 2013, **49**, 274–279.
54 M. A. Ziganshin, A. V. Yakimov, G. D. Safina, S. E. Solovieva, I. S. Antipin and V. V. Gorbatchuk, *Org. Biomol. Chem*., 2007, **5**, 1472–1478.
55 A. Kelly and K. M. Knowles, *Crystallography and Crystal Defects*, Chichester, John Wiley & Sons Ltd., 2012.